Chinese Chemical Letters 33 (2022) 3623–3631

Contents lists available at ScienceDirect

Chinese Chemical Letters

journal homepage: www.elsevier.com/locate/cclet

Recent progress in carbon-based materials boosting electrochemical water splitting

Ziqi Zhang[a], Yin Lei[a], Weimin Huang[a,b,c,*]

[a] College of Chemistry, Jilin University, Changchun 130012, China
[b] Key Laboratory of Physics and Technology for Advanced Batteries of Ministry of Education, Jilin University, Changchun 130012, China
[c] School of Pharmaceutical Sciences, Jilin University, Changchun 130012, China

ARTICLE INFO

Article history:
Received 13 September 2021
Revised 12 October 2021
Accepted 13 November 2021
Available online 18 November 2021

Keywords:
Carbon-based materials
Water splitting
Electrocatalysis
Carbon neutrality
Hydrogen evolution reaction
Oxygen evolution reaction

ABSTRACT

As environmental crises such as global warming become more and more serious due to the large amount of carbon dioxide emitted by the burning of fossil fuels, much attention has been paid to carbon neutrality. Hydrogen, with zero carbon content, is a clean and renewable energy carrier having a large energy density. It is considered as one of the most desirable alternatives to fossil fuels. Electrochemical water splitting, unlike the steam reforming process accelerating fossil fuels depletion and CO_2 emissions, can produce H_2 powered by renewable energy such as solar or wind. As a promising way to promote carbon neutralization, hydrogen production by electrolysis of water is meaningful both in terms of scientific research and practical application. In order to drive electrochemical water splitting with low power consumption, efficient, durable and affordable electrocatalysts with low overpotentials are in urgent need. Therefore, this mini-review briefly introduces the current development status and mainstream obstacles of carbon-based materials used in electrochemical water splitting.

1. Introduction

With the growth of population and the development of industry in modern society, more and more fossil fuels are consumed, resulting in massive carbon dioxide emissions [1,2]. The increasing global environmental crisis arouses more and more attention to greenhouse effect [3], which increased the emphasis on renewable sources conversion and storage [4,5]. It is necessary to develop new and renewable energy sources to replace fossil fuels in order to reduce CO_2 emission effectively [6,7]. Hydrogen, with zero carbon content, is a clean and renewable energy carrier having a large energy density [8], which is considered as one of the most desirable alternatives to fossil fuels [9,10] by virtue of its high energy density, carbon neutral and environmental friendliness, *etc.* [11,12]. However, the most mainstream way to produce hydrogen nowadays is steam reforming process, which accelerates fossil fuels depletion and CO_2 emissions [13]. Therefore, electrochemical water splitting, as an alternative way to produce H_2 of high-purity [14], is drawing more and more attention since it can produce H_2 powered by renewable energies, *e.g.*, solar or wind [15,16].

In order to drive electrochemical water splitting with low power consumption, efficient, durable and affordable electrocatalysts with low overpotentials towards hydrogen evolution reaction (HER) [17,18] and oxygen evolution reaction (OER) [19–22] are in urgent need. According to recent researches, the most mainstream catalysts are metal-nonmetal complexes [23], including metal oxides [24], sulfides [25–27], phosphides [28–30], carbides [31] and nitrides [32]. Among them, Carbon-based materials exhibit superior properties in photocatalysis [33,34] and electrocatalysis [35] due to the synergistic effects between doped metal atoms and carbon support. Carbon supports can not only provide solid anchor sites for metal atoms, but also regulate the coordination environment of metal atoms so that they can have more favorable binding energy towards reactants [36–38]. Furthermore, according to the types of metal atoms in carbon materials, we can divide them into noble metal catalysts and non-noble metal catalysts [39]. On the one hand, noble metals such as platinum (Pt), iridium (Ir), ruthenium (Ru) are used as benchmark electrocatalysts towards electrochemical water splitting thanks to their high efficiency and stability [40,41]. However, the high cost and low abundance greatly limit the further use of noble metal electrocatalysts [42]. On the other hand, low-cost and earth-abundant electrocatalysts such as carbon-based Fe, Co and Ni materials are difficult to replace noble metal catalysts within a short period due to un-

* Corresponding author at: College of Chemistry, Jilin University, Chanchun 130012, China.
E-mail address: huangwm@jlu.edu.cn (W. Huang).

https://doi.org/10.1016/j.cclet.2021.11.041
1001-8417/

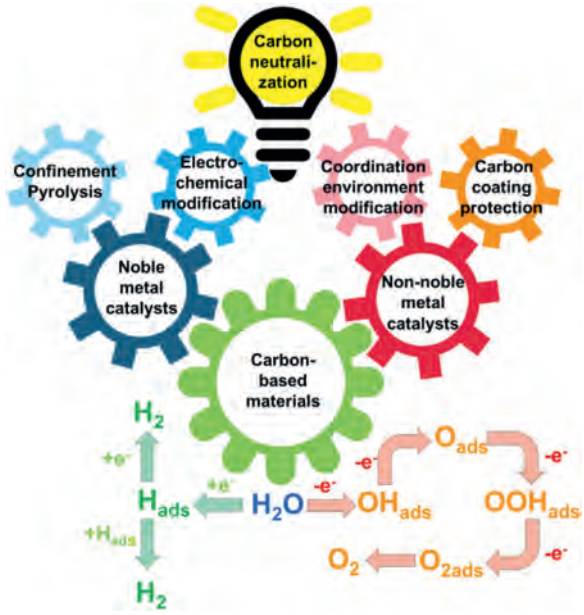

Fig. 1. General strategies to optimize the carbon-based materials towards electrochemical water splitting.

satisfactory stability, high overpotential and excessive load [43,44]. In conclusion, it is obvious that both noble metal catalyst and non-noble metal catalyst have their unique advantages and disadvantages. How to modify carbon-based materials according to the characteristics of noble metal catalysts and non-noble metal catalysts in order to maximize their catalytic performance and reduce the cost is currently attracting the most attention of researchers [13,23,45,46].

In this mini review, we summarized the innovative methods for preparing carbon-based materials towards electrochemical water splitting. These methods generally can be divided into two strategies (Fig. 1). One is to increase the utilization rate of noble metal atoms by using the carbon base as a stable and conductive platform to disperse noble metal atoms so as to reduce the cost without weakening the catalytic performance. The other is to boost the catalytic performance and stability of non-noble metal catalysts by modifying the interactions between carbon bases and non-noble metal atoms [47], which provides a possibility to replace noble metal catalysts in the future [48]. The review will introduce the current state of development, the problems encountered and corresponding solutions of carbon-based materials towards electrochemical water splitting.

2. Strategies to optimize the noble metal catalysts

Noble metal materials are the most active electrocatalysts for catalyzing water splitting [49]. Although noble metals such as Pt [50–52], Ir [19,20,53] and Ru [39,54] are used as mainstream water splitting electrocatalysts for their high intrinsic activity and satisfactory stability, their high cost and low abundance hinder their further applications [55]. Therefore, for noble metal catalysts, how to reduce their dosage without damaging their excellent catalytic performance has always been a hot research topic [20,54]. At present, the most popular method is to disperse noble metal atoms or nanoparticles evenly into carbon-based materials to greatly improve the atomic utilization rate of noble metal in catalysts [42,56]. Herein, we present two representative approaches to obtain highly dispersed noble metal modified carbon-based materials. One is to confine noble metal atoms into porous materials [57] or surface vacancies [58], such as metal-organic frame (MOF) [59] or covalent organic framework (COF) [60], and then form stable metal-carbon bonds by high-temperature pyrolysis. The stability of chemical bonds can overcome the high surface free energy of highly dispersed noble metal atoms [61]. The other is to use electrochemical modification method to anchor noble metal atoms uniformly on the surface of carbon material precursor by the force of the electric field [51,52,62,63].

2.1. Confinement Pyrolysis

Theoretically, the higher the dispersion of noble metal atoms in the catalyst, the higher the utilization rate of noble metal atoms [64,65]. For example, single-atom catalysts have a metal dispersibility of nearly 100% and unique metal coordination environments [66], which provide the maximum atom use efficiency and unique catalytic properties that differ from those of bulk catalysts [67,68]. However, due to the excess surface free energy [69,70], noble metals with small size (single atoms or nanoparticles) tend to aggregate into larger particles during the pyrolysis process [71,72]. This can lead to extreme degradation or even deactivation of the catalyst, which can have a fatal effect on the utilization rate of noble metals [73,74]. On the one hand, forming strong metal-support interactions or ligands to thermodynamically stabilize metal atoms are effective approaches to reduce the surface energy and the tendency of metal atom migration [75,76]. On the other hand, confining the metal atoms within microporous solids can kinetically prevent the collision and coalescence of noble metal atoms or nanoparticles [77–79].

Li *et al.* report the successful reversion of sintering effects and the conversion of noble metal nanoparticles into thermally stable highly active single atoms (Pd, Pt, Au) fixing in the carbon-based material [67]. They utilized nitrogen-doped carbon (CN) derived from a MOF (zeolite imidazolate framework-8, ZIF-8) [80,81] as the anchoring substrate to capture the migrating metal atoms at high temperatures. Furthermore, they use *in situ* environmental transmission electron microscopy (ETEM) to observe the process of noble metal single atoms being anchored on carbon-based materials. It can be seen intuitively that sintering occurs and larger Pd nanoparticles will form at high temperatures at first. However, the enlarged Pd-NPs would intensively collide with the substrate, gradually become smaller and finally transform to single atoms. The obtained thermally stable Pd-SAs showed even better catalytic activity and selectivity than Pd-NPs for semi-hydrogenation of acetylene. This is the first reported *in situ* observation of an entire process that noble metal single atoms anchored to a carbon material at high temperatures, which provides an intuitive and clear explanation for the mechanism of fixing noble metals atoms on carbon-based materials by confinement pyrolysis method. Specifically, it is not the bond energy of metal-nonmetal coordination bonds formed between metal atoms and carbon precursors at room temperature that enables metal atoms to overcome the high surface free energy that tends to agglomerate at high temperatures. Instead, the metal atoms aggregate in the carbon-based material during the confinement pyrolysis process at first, and then the chemical bonds formed by the irregular collision between the metal aggregations and the carbon-based material during the following pyrolysis process stabilize the metal atoms. Over time, the metal aggregates gradually become smaller and finally disappear, forming more and more single atoms anchored on the nitrogen-doped carbon matrix, eventually forming stable, highly dispersed noble metal single atomic carbon-based materials. Similarly, Huang *et al.* demonstrated a new low-noble metal electrocatalyst for HER, which was obtained by direct carbonizing Ru doped ZIF-8-based nitrogen carbon mixture (Ru@NC) [39]. The Ru@NC was synthesized by one-pot method and was calcined in high temperature and in nitrogen atmosphere to acquire Ru embedded N-doped carbon framework

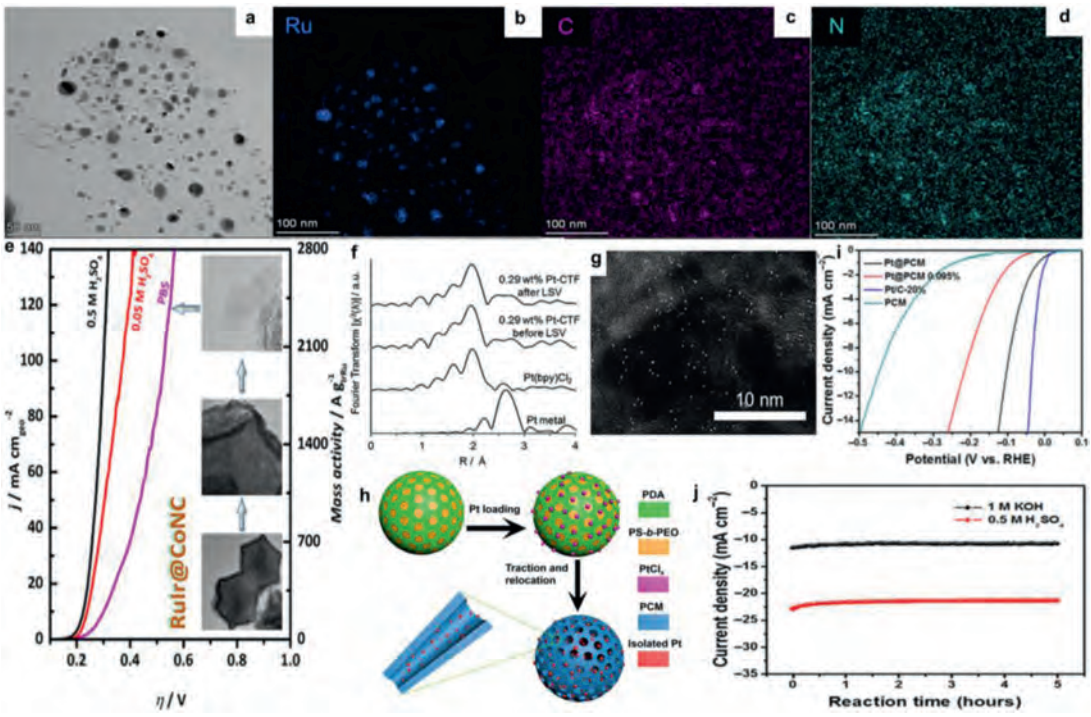

Fig. 2. (a) HAADF-STEM image, (b-d) corresponding EDS mapping images Ru@NCF. Reproduced with permission [39]. Copyright 2020, Elsevier. (e) OER activities of RuIr@CoNC in 0.5 mol/L H_2SO_4, 0.05 mol/L H_2SO_4, and PBS electrolytes, respectively. Inset are TEM images taken at different magnifications and HRTEM images of RuIr@CoNC. Reproduced with permission [94]. Copyright 2021, The American Chemical Society. (f) Fourier transformations of k^3-weighted Pt L_3-edge EXAFS oscillations and (g) the corresponding HAADF-STEM image of Pt-CTF. Reproduced with permission [60]. Copyright 2016, John Wiley and Sons. (h) Schematic illustration of the synthetic procedure of Pt@PCM. (i) LSV curves of various catalysts in 0.5 mol/L H_2SO_4. (j) *I-t* curves of Pt@PCM in 1 mol/L KOH and 0.5 mol/L H_2SO_4 media at a bias of 0.15 V *versus* RHE. Reproduced with permission [103]. Copyright 2018, American Association for the Advancement of Science.

(Ru@NCF) (Figs. 2a-d). The carbonized Ru@NC provides high surface area and satisfying stability with 0.39 wt% loading of Ru. This indicates that MOF can be used as a very ideal carrier for the dispersion of noble metal atoms or nanoparticles.

Ruthenium and iridium-based materials are the best electrocatalysts known to date that show reasonably good OER performance in strongly acidic electrolyte [82–87], which have been continuously attracting great research interest [88–93]. Liu *et al.* design a catalyst comprising surface atomic-step enriched ruthenium-iridium (RuIr) nanocrystals homogeneously dispersed on a MOF derived carbon support (RuIr@CoNC) (Fig. 2e), which shows outstanding catalytic performance for OER with high mass activities of 2041, 970 and 205 A/g_{RuIr} at an overpotential of 300 mV and can sustain continuous OER electrolysis up to 40, 45, and 90 h at 10 mA/cm^2 with minimal degradation in 0.5 mol/L H_2SO_4 (pH 0.3), 0.05 mol/L H_2SO_4 (pH 1), and PBS (pH 7.2) electrolytes, respectively [94]. On one hand, to the presence of abundant atomic steps that maximize the exposure of catalytically active sites and lower the limiting potential of the rate-determining step of OER and, on the other hand, to the strong interaction between RuIr nanocrystals and the CoNC support that endows homogeneous dispersion and firm immobilization of RuIr catalysts on CoNC. The RuIr@CoNC catalysts also show outstanding performance in a single-cell PEM electrolyzer, and their large-quantity synthesis is demonstrated.

In addition to MOF, COF is also used as an ideal carbon-based material for loading noble metal single atoms [95–97] or particles [98–100]. Nakanishi *et al.* reported that covalent triazine frameworks (CTFs) can serve as a platform for single-atom electrocatalysts [60]. Although CTFs are non-conductive, they successfully developed a CTF-based electrocatalyst by hybridizing CTFs with conductive carbon particles [98]. As CTFs possess abundant nitrogen atoms with an electron lone pair, various metals can be loaded onto CTFs by coordination bonds with nitrogen [101]. Using this approach, atomic Pt-modified CTFs (Pt-CTF) exhibit unique reaction activity and selectivity towards HER. It can be seen clearly that no Pt aggregates were detected in the Fourier transformations of k^3-weighted EXAFS oscillations (Fig. 2f) or by high-angle annular dark-field scanning transmission electron microscopy (Fig. 2g), which indicates that platinum single atoms have been successfully loaded on CTF. Notably, Pt-CTF also exhibited high oxygen tolerance, which is critical for limiting cathode degradation during the start-stop cycles of fuel cells. This also shows that noble metal atoms dispersed on COF can achieve some unexpected selectivity, and provides a guiding idea for subsequent design of electrocatalysts.

A porous carbon matrix (PCM) with high conductivity, good stability, and confined microenvironment is considered as an ideal support to stabilize isolated Pt centers for electrocatalysis [102]. However, Pt single atoms loaded by the traditional wet-chemistry approach are hardly confined into the PCM. This is caused by the charge-balancing double layer generated from cationic or anionic precursors, which prevents the diffusion of Pt component into the interior of the porous matrix [68]. Lou *et al.* report a novel dynamic reaction approach for traction and stabilization of isolated Pt atoms in the PCM (Pt@PCM) through the relocation of the single-atom Pt species from the surface of the parent carbon sphere into the interior of the carbon matrix as a highly active and stable electrocatalyst toward HER [103]. Schematic illustration of the synthetic procedure of Pt@PCM was shown in Fig. 2h. Mesostructured polydopamine (PDA) particles, integrated with the Pt component, are innovatively used as the precursor for the synthesis of Pt@PCM. Pyrolysis of the precursor generates mesopores, owing to the decomposition of the surfactants in the PDA particles. Meanwhile, the internal dynamic force, as a consequence of the mesopore formation and high-temperature pyrolysis, progressively fuses Pt ions into the crystal lattice of PCM, generating the Pt@PCM electrocatalyst with high dispersity of active centers. The onset potential of Pt@PCM is comparable with that of Pt/C (Fig. 2i). The Pt@PCM requires small

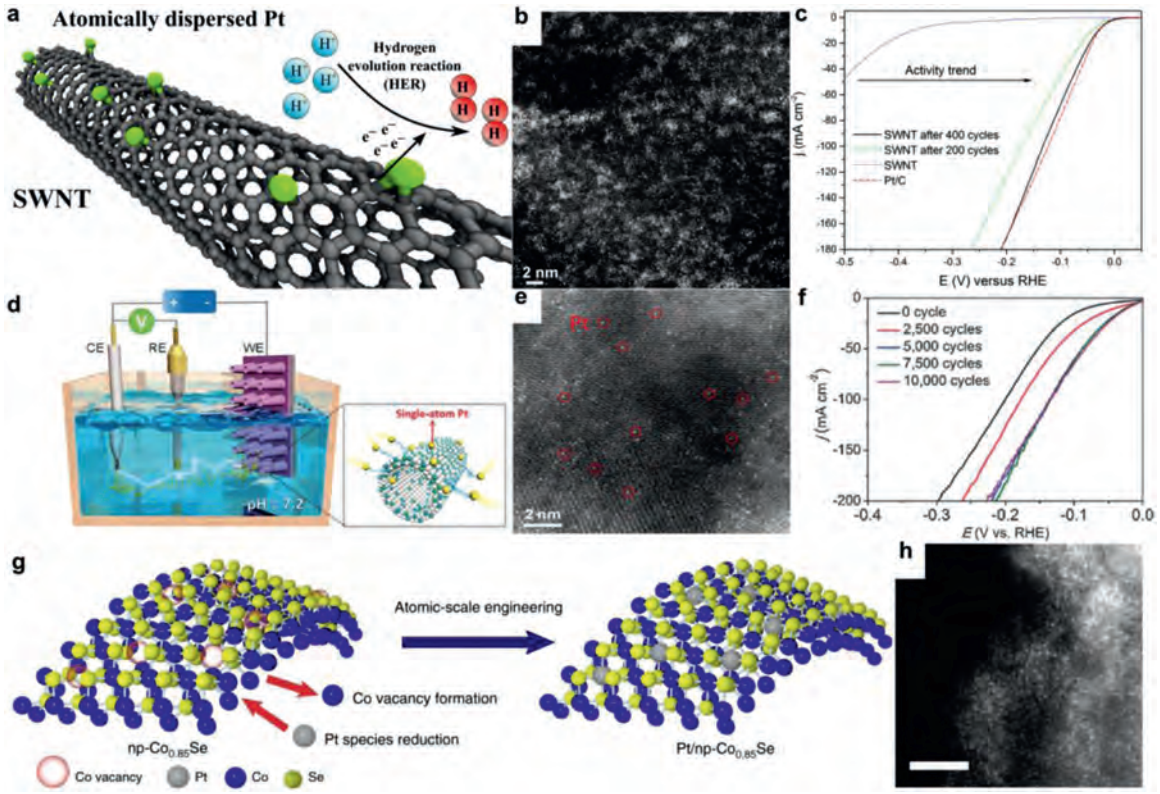

Fig. 3. (a) Illustration of the SWNT/Pt. (b) HAADF images from an ultrathin film of activated SWNT/Pt deposited on a TEM grid. The HAADF images show the uniform atomic dispersion of Pt (mainly single atoms, two-dimensional Pt rafts, and small clusters) on the SWNT. (c) HER polarization curves of SWNT (blue), Pt/C (red), and SWNT activated with 200 (green) and 400 (black) activation cycles. (a-c) Reproduced with permission [110]. Copyright 2017, The American Chemical Society. (d) Schematic diagram of the synthesis process of PtSA-NT-NF. (e) Atomic-resolution (AR) HAADF image of the PtSA-NT-NF (Pt atoms ringed in red). (f) HER polarization curves of the PtSA-NT-NF precursor sample after different numbers of potential cycles were performed on it. (d-f) Reproduced with permission [114]. Copyright 2017, John Wiley and Sons. (g) Schematic illustration of the fabrication procedure of Pt/np-$Co_{0.85}Se$. (h) HAADF-STEM images of Pt/np-$Co_{0.85}Se$, Scale bars: 2 nm. (g, h) Reproduced with permission [51]. Copyright 2019, Nature Publishing Group.

overpotentials of 105 and 142 mV to achieve current densities of 10 and 20 mA/cm^2, respectively. Moreover, the electrochemical stability of Pt@PCM in acidic and alkaline media are both satisfactory as shown in Fig. 2j.

2.2. Electrochemical modification

The electrochemical modification method has been reported to prepare highly dispersed noble metal modified carbon-based materials [52]. Compared with pyrolysis method, electrochemical method is mild and controllable [104]. Unlike pyrolytic materials, it does not have to overcome the high surface free energy of highly dispersed noble metal atoms dispersed among the surface of carbon-based materials [105]. It does not require complex and expensive noble metal salt electrolyte, too [106]. Only a noble metal electrode needs to be used as the counter electrode (CE), and the carbon-based material precursor is coated on the surface of working electrode (WE) [107]. The electrochemical workstation can realize the modification at room temperature and normal pressure [108]. Platinum is dissolved in sulfuric acid at voltages exceeding the Pt dissolution onset potential of *ca.* 1.1 V *vs.* RHE [109]. Then, a cathodic growth of platinum particles [110] or single atoms [50-52,111-114] on carbon-based materials (working electrode) can be easily triggered by anodic dissolution of platinum from a Pt electrode in acidic media [62].

For example, Yao *et al.* reported a distributed atomic Pt-Co nitrogen-carbon-based catalyst *via* electrochemical modification method. Analogously, Laasonen *et al.* anchored atomic-scale platinum on the sidewalls of single-walled carbon nanotubes (SWNT/Pt) [110] in a three-electrode cell setup in 0.5 mol/L H_2SO_4 (Fig. 3a). The activation was done *via* potential cycling of an SWNT-coated glassy-carbon (GC) electrode as the working electrode (WE) between −0.55 V and 0.25 V *vs.* the reversible hydrogen electrode (RHE), while a Pt foil was utilized as the counter electrode (CE). Once the potential applied on the WE was decreased to −0.55 V, the potential applied on the CE increased to *ca.* 2.2 V. When the potential on the CE exceeds the dissolution onset potential of 1.1 V for Pt in acidic media, Pt species (Pt^{2+} or Pt^{4+}) are dissolved from the Pt electrode into the electrolyte and subsequently reduced on the WE [62,109]. As shown in Fig. 3b, the HAADF image shows the uniform atomic dispersion of Pt (mainly single atoms, two-dimensional Pt rafts, and small clusters) on the SWNTs after CV. And the SWNT/Pt after 400 segments of CV exhibits low overpotentials of 27, 130, and 210 mV to achieve current densities of 10, 100, and 180 mA/cm^2, respectively (Fig. 3c), which are similar to those of Pt/C. Most importantly, the SWNT/Pt after 200 and 400 segments of CV contains 0.19 and 0.75 atom % of Pt. This indicates that the electrochemical modification method successfully anchors highly dispersed platinum atoms into the SWNTs, which can greatly improve the atomic utilization rate and reduce the cost of noble metal catalyst.

Luo *et al.* demonstrate a potential-cycling method to synthesize a catalyst comprising single Pt atoms on CoP-based carbide nanotube arrays supported by a Ni foam (PtSA-NT-NF) (Fig. 3d) [114]. In PBS, it exhibits an ultralow overpotential (η) of 24 mV for the HER current density (j_{HER}) of 10 mA/cm^2, only 7 mV larger than that of commercial Pt/C. Briefly, in a three-electrode cell containing 1 mol/L PBS (pH 7.2), a Pt foil, a saturated calomel electrode (SCE),

and a NF with transition metal carbide precursors are employed as CE, RE, and WE, respectively. Cyclic voltammetry was performed with the scan rate of 150 mV/s between −1.5 V and −0.668 V *vs.* SCE at 25°C. Fig. 3e exhibits that the platinum single atoms were uniformly dispersed on the surface of transition metal carbon materials by electrochemical cyclic voltammetry. It can be seen clearly in Fig. 3f that the HER electrocatalytic performance of WE and its corresponding structure changed during the first 5000 cycles. After the 5000 cycles, the changing trend faded, suggesting that the structure of WE became stable.

Tan *et al.* reported single-atom platinum decorated nanoporous $Co_{0.85}Se$ (Pt/np-$Co_{0.85}Se$) as efficient electrocatalysts for hydrogen evolution [51]. The achieved Pt/np-$Co_{0.85}Se$ shows high catalytic performance with a near-zero onset overpotential, a low Tafel slope of 35 mV/dec, and a high turnover frequency of 3.93 s^{-1} at −100 mV in neutral media, outperforming commercial Pt/C catalyst. The catalyst was prepared by an electrochemically selective etching method [115] combined with depositing Pt atom on working electrode. Electrochemical vacancy manufacturing and Pt atom embedding were conducted by cyclic voltammetry (CV) using Pt foil as counter electrode in a three-electrode cell containing 0.5 mol/L H_2SO_4. As shown in Fig. 3g, during the cyclic process, slight Co atoms dissolved from the np-$Co_{0.85}Se$ to form Co vacancies, thus providing anchor sites for the embedding of Pt. As Fig. 3h shown, single-atom Pt appearing as bright spots can be found to be well dispersed in the lattice of $Co_{0.85}Se$, confirming the formation of single-atom dispersed catalyst.

Furthermore, besides platinum (Pt), palladium (Pd), rhodium (Rh) and gold (Au) electrodes have also been used to investigate dissolution under acidic conditions [116]. However, there have been few reports about the Pd, Ru or Au dispersed on carbon-based electrocatalysts *via* electrochemical modification. This is probably because they have no advantage over platinum in terms of processing difficulty and versatility. However, we believe that the electrochemical modification mentioned in this section is a general method. These noble metals can also be uniformly deposited on the carbon-based materials at the working electrode using this simultaneous dissolving-deposition process. This provides a wider choice for us to produce the highly dispersed noble metal carbon-based materials by electrochemical modification method.

3. Strategies to optimize the non-noble metal catalysts

Although noble metal materials show excellent performance towards electrochemical water splitting, the scarcity and high price of Pt restrict their large-scale application [117–120]. Therefore, the development of efficient, low-cost, and environmentally friendly catalysts for the electrochemical water splitting is necessary [121]. Various transition-metal carbon-based electrocatalysts have been applied to replace noble metal catalysts [122,123]. However, compared with stable and efficient noble metal catalysts, the performance and endurance of non-noble metal catalysts are not satisfactory [115,124,125]. Once these two shortcomings can be overcome, the substitution of noble metal catalysts can be realized, which will be a major breakthrough for electrochemical water splitting and promote its further practical application. Herein, two representative methods are introduced. One is to improve the intrinsic catalytic activity of non-noble metal carbon materials by regulating the coordination environment of non-noble metal in the carbon substrate so that it has the moderate adsorption energy comparable to that of noble metal towards reaction intermediate of electrochemical water splitting. Another strategy is to form a robust conductive carbon layer on the catalyst surface through other auxiliary substances such as surfactants, so as to greatly enhance the durability of non-noble metal materials. These two methods are the most mainstream ways to overcome the shortcomings of non-noble metal carbon-based materials in unsatisfactory performance and poor stability.

3.1. Coordination environment modification

Long before the concept of single-atom catalysts (SACs) was proposed, nature-inspired molecules like porphyrin, phthalocyanines, and organometallic complexes were popular as heterogeneous catalysts for various reactions [126]. The M−N_x centers in M−N−C materials play the role of the active sites for ORR and HER since they can facilitate the adsorption of OOH* and H* intermediates during these reactions [127–130]. On the one hand, this unique metal-nitrogen-carbon (M−N−C) structure can regulate the coordination environment of the central metal atom, so that it has a more ideal electronic structure and adsorption energy towards reactant. On the other hand, the M−N−C structure can provide a strong metal-carbon based interaction through chemical bonds, which can ensure the stability of the metal atom in the catalytic process [64,131]. Considering these features, several approaches were investigated to derive the rational design of non-noble metal carbon-based materials with a balanced coordination environment to improve their catalytic performance. Here, Huang *et al.* report a general approach to a series of monodispersed atomic transition metals (for example, Fe, Co, Ni) embedded in nitrogen-doped graphene with a common MN_4C_4 moiety, identified by systematic X-ray absorption fine structure analyses and direct transmission electron microscopy imaging [132]. The unambiguous structure determination allows density functional theoretical prediction of MN_4C_4 moieties as efficient oxygen evolution catalysts with activities following the trend Ni > Co > Fe, which is confirmed by electrochemical measurements. Determination of atomistic structure and its correlation with catalytic properties represents a critical step towards the rational design and synthesis of non-noble metal carbon-based catalysts with exceptional stabilities and catalytic activities.

Huang *et al.* demonstrated that the Co-based MOF (ZIF-67) anchoring on an indium-organic framework (InOF-1) composite (InOF-1@ZIF-67) is treated followed by carbonization and phosphorization to successfully obtain CoP nanoparticles-embedded carbon nanotubes and nitrogen-doped carbon materials (CoP-InNC@CNT) (Fig. 4a) [133]. As shown in Fig. 4b, X-ray photoelectron spectroscopy was applied to investigate the types and chemical states of the surface element. It demonstrates the formation of Co−P and C−P bonds. This indicates that the addition of P element not only changes the coordination environment of metal active center Co, but regulates the arrangement of N−C matrix, ultimately improving the intrinsic activity of CoP-InNC@CNT catalyst, and eventually achieving a more effective electrochemical water splitting process. As HER and OER electrocatalysts, it is demonstrated that CoP-InNC@CNT simultaneously exhibit high HER performance (overpotential of 153 mV in 0.5 mol/L H_2SO_4 and 159 mV in 1.0 mol/L KOH) and OER performance (overpotential of 270 mV in 1.0 mol/L KOH) activities to reach the current density of 10 mA/cm^2 (Fig. 4c). In addition, these CoP-InNC@CNT rods, as a cathode and an anode, can display an excellent OWS (overall water splitting) performance with $\eta_{10} = 1.58$ V and better stability, which shows the satisfying electrocatalyst for the electrochemical water splitting. The TEM and corresponding EDS mapping images for CoP-InNC@CNT rods are shown in Fig. 4d, indicating that elements are evenly distributed on the surface of the material. This work initiates a coordination environment modification strategy to synthesize CoP-loaded nitrogen-doped carbon composite with fine structure. Furthermore, the present work can be readily extended to offer the cost-effective, energy-efficient, and bifunctional electrocatalysts for performance enhancements of non-noble metal carbon-based catalysts.

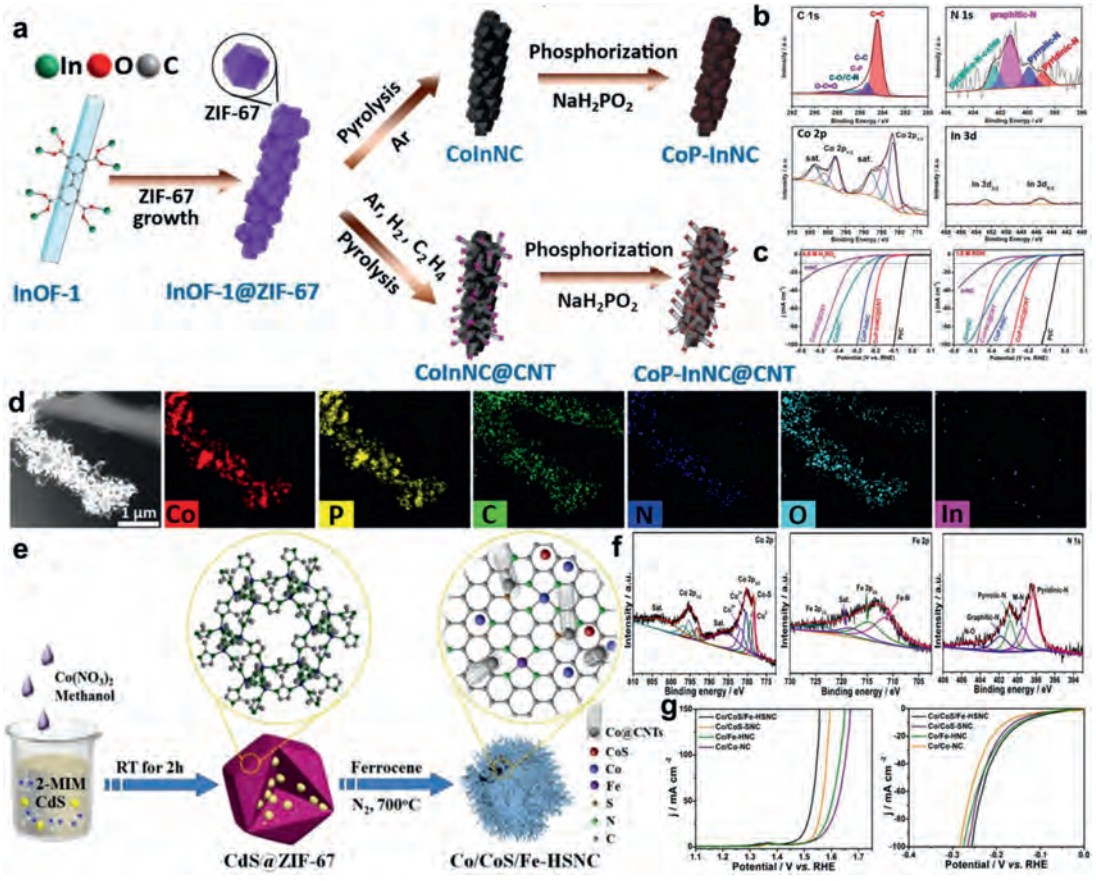

Fig. 4. (a) Schematic illustration of the synthetic process for CoP-InNC and CoP-InNC@CNT composites. (b) Deconvoluted XPS spectra for CoP-InNC@CNT rods. (c) LSV curves of CoP-InNC@CNT and control samples in 0.5 mol/L H_2SO_4, 1.0 mol/L KOH for HER. (d) The TEM and corresponding EDS mapping images for CoP-InNC@CNT rods. (a-d) Reproduced with permission [133]. Copyright 2020, John Wiley and Sons. (e) Schematic illustration of the synthetic route of the Co/CoS/Fe-HSNC. (f) High-resolution Co 2p, Fe 2p and N 1s XPS spectra of the Co/CoS/Fe-HSNC. (g) OER performances and HER performances of the as-prepared Co/CoS/Fe-HSNC and other samples. (e-g) Reproduced with permission [134]. Copyright 2021, Elsevier.

With the introduction of CdS and ferrocene, Hu *et al.* report a MOF-induced strategy to synthesize a hierarchical trifunctional electrocatalyst based on Co/CoS nanoparticles and metal (Co,Fe)−N−C species in a hairy S,N-codoped mesoporous carbon polyhedron interwoven with carbon nanotubes (Co/CoS/Fe-HSNC) (Fig. 4e) [134] for water splitting. CdS nanoparticles is demonstrated to act as a pore former and S sources both for reaction and doping (Fig. 4f), and ferrocene is employed to initiate the *in-situ* growth of carbon nanotubes and Fe−N−C active sites which both contribute to superior multifunctional activities (Fig. 4g). Although the current OER and HER activities of the M−N−C catalysts are not satisfactory [135,136], which seriously hinders their applications in metal-air batteries and water splitting. This work introduces S into M−N−C structure to regulate the coordination environment of the active center of Fe and Co metals for enabling the catalyst with multifunctionality for the ORR, OER and HER [137]. This is an excellent example of coordination environment modification strategy in practical application, which provides new insight into the construction of M−N−C derived non-noble metal carbon-based catalysts for water electrolysis.

3.2. Carbon coating protection

Coordination environment modification method mainly focuses on the insufficient performance of non-noble metal catalysis while carbon coating protection strategy is principally applied to enhance the durability of non-noble metal catalysts. Unlike the noble metal catalyst with satisfactory stability, non-noble metal catalysts have been suffering from poor stability due to the leaching of the non-precious metal sites from catalysts [138–141], the attack by H_2O_2 (and/or free radicals) [142] and protonation of the active site or adjacent N dopants followed by anion adsorption [143]. Stability is the biggest challenge for the practical application of non-noble metal electrocatalysts towards water splitting especially OER. Herein, in this section, we introduce several representative methods to improve the stability of non-noble metal catalysts by constructing a conductive, stable carbon coating structure covering the catalyst.

Simply increasing Co metal content in the precursors is found to be ineffective because it gives rise to severe aggregation of Co metal during high-temperature treatments [144]. Thus, new strategies to effectively control the synthesis of CoN_x active sites with high density are extremely desirable, but very challenging. Wu *et al.* developed an innovative surfactant-assisted MOF approach to preparing core-shell structured Co–N–C catalysts (Co–N–C@F127) [145], which was inspired by the strong interactions between surfactants and nanocrystal particles in solution phases [146–148]. Due to the confinement role of surfactants (F127) covering onto the Co-ZIF-8 nanocrystals, core-shell structured and atomically dispersed Co–N–C@surfactant catalysts with significantly increased active site density were obtained. Furthermore, after pyrolysis, the F127 in the outer layer of Co-ZIF-8 spontaneously forms a regular carbon thin layer that protects the internal CoN_4 site without decreasing mass transfer ability and electrical conductivity. Based on HR-TEM and HAADF-STEM images (Figs. 5a-d) the carbon networks in both Co–N–C and Co–N–C@F127 catalysts were highly disor-

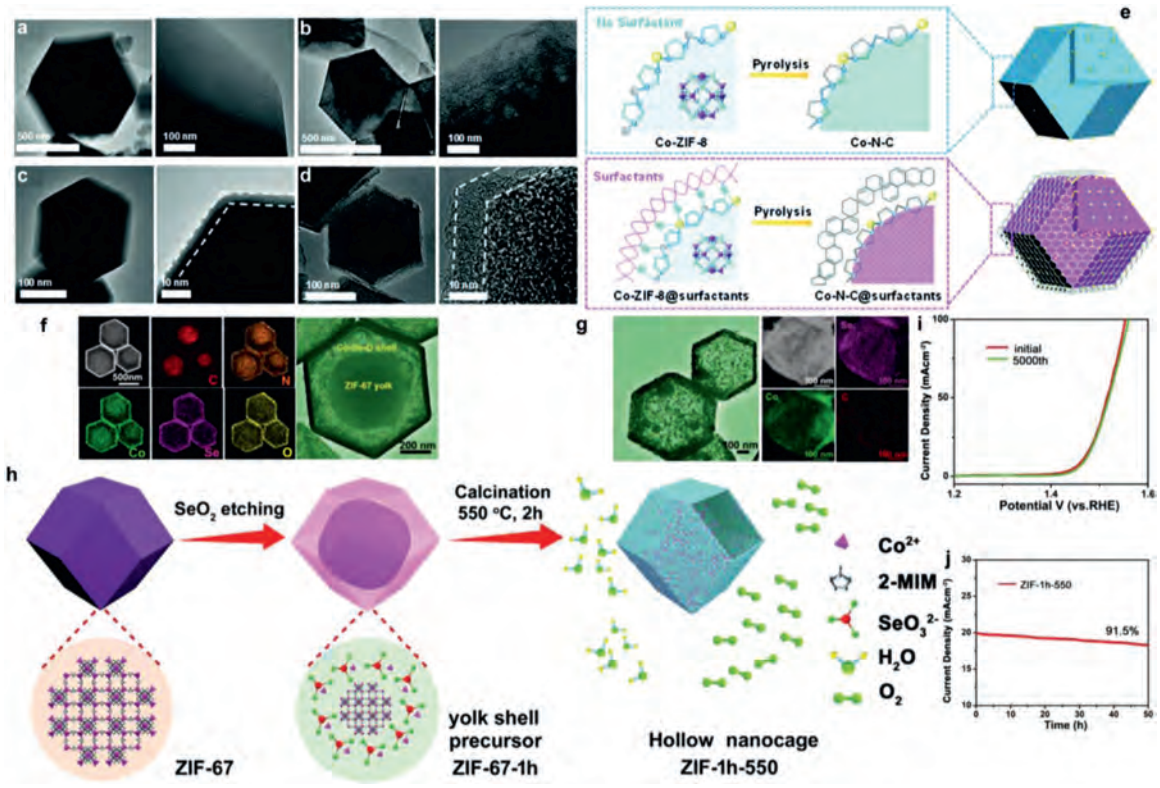

Fig. 5. HRTEM and HAADF-STEM for (a) surfactant-free Co-ZIF-8 precursor, (b) Co-ZIF-8@F127 precursor, (c) surfactant-free Co–N–C catalyst and (d) Co–N–C@F127 catalyst. (e) Schematic illustration of *in situ* confinement pyrolysis strategy to synthesize core-shell-structured Co–N–C@surfactants catalysts. The yellow, grey and blue balls represent Co, Zn and N atoms, respectively. (a-e) Reproduced with permission [145]. Copyright 2018, the Royal Society of Chemistry. (f) TEM images and EDS elemental mapping of C, N, Co, Se, O elements of $Co_{0.85}Se_{1-x}$@C precursors. (g) TEM images and EDS Elemental mapping of C, Co, Se elements of $Co_{0.85}Se_{1-x}$@C. (h) Schematic illustration of the routes to $Co_{0.85}Se_{1-x}$@C hollow nanocages with rich Se vacancy. (i) Polarization curves for $Co_{0.85}Se_{1-x}$@C before and after 5000 cycles. (j) *I-t* curve for $Co_{0.85}Se_{1-x}$@C at the η_{20} for 50 h. (f-j) Reproduced with permission [151]. Copyright 2021, John Wiley and Sons.

dered due to the doping of the heteroatoms N, which led to the turbostratic stacking of graphite planes [149]. Notably, the Co–N–C@F127 exhibited a typical core-shell structure, in which the core was derived from the Co-doped ZIF-8 nanocrystal and the carbon shell was from the surfactant layers (Fig. 5e) [150]. The partially graphitized carbon shells could be clearly observed at the edge of the polyhedron, attributable to the graphitization of F127. Compared to the carbon structures in the shells, the carbon cores derived from the ZIF-8 precursors seem more amorphous and porous. In conclusion, surfactant-assisted confinement pyrolysis strategy can not only enable controlled synthesis of atomically dispersed CoN_4 sites with increased density, therefore leading to significantly enhanced catalytic activity. This carbon shell derived from surfactant layer can also effectively retain dominant micropores and high content of N in the carbon matrix as well as protect the active sites inside the carbon layer from acidic or alkaline solution, thus preventing the agglomeration or leaching out of single atomic Co sites. The surfactant-assisted confinement strategy provides a new approach to synthesizing non-noble metal catalyst with significantly increased stability for widespread electrochemical energy conversion applications.

In addition to surfactant-assisted confinement strategy, another general method for fabricating carbon coating layer structures has recently been proposed. Hu *et al.* reported a general, selenic-acid-assisted etching strategy from a metal-organic framework as a precursor to realize carbon-coated 3D metal selenides $Co_{0.85}Se_{1-x}$@C nanocages with rich Se vacancies as high-performance non-noble metal electrocatalyst which delivers an overpotential of only 231 mV at a current density of 10 mA/cm^2 for the OER and the corresponding full water-splitting electrolyzer requires only a cell voltage of 1.49 V at 10 mA/cm^2 in alkaline media [151]. The selenic acid partially etches ZIF-67 framework and also acts as a source of selenium under a mediate condition. Finally, carbon layer-coated $Co_{0.85}Se_{1-x}$@C derivatives were obtained after a subsequent calcination at intermediate temperature under inert atmosphere. Compared with the conventional one-step calcination method [152,153], the selenic-acid-assisted etching strategy can not only introduce rich Se vacancies into the $Co_{0.85}Se_{1-x}$@C hollow structures, which gives rise to a great increase in the number of active sites, enhancement of the electronic conductivity, and thereby decreased energy barrier for the formation of intermediates, consequently significantly improved catalytic activity for OER in a strong alkaline medium was observed. Most importantly, it can also form carbon-coated layers around the nanocage structures which can serve as a barrier to protect the active sites inside the nanocages from corrosion and damage caused by strong alkaline conditions (Figs. 5f-h). Therefore, even under continuous OER operation, the activity was not largely affected (Figs. 5i and j). This work provides a new opportunity to realize high-performance OER electrocatalysts by a general strategy on carbon-coated 3D metal selenides nanocages.

Besides surfactant-assisted approach and selenic-acid-assisted etching strategy, electrochemical water splitting catalysts with protective carbon-coating structure can also be synthesized by direct pyrolysis. Huang *et al.* synthesize the Fe–Ni bimetallic N-doped carbon framework (Fe–Ni@NCF) towards HER in both alkaline and acidic conditions [9]. It exhibits less current density loss compared to commercial Pt/C after stability test which exhibits better endurance. This is mainly because the Fe–Ni nanoparticles are wrapped and connected by N-doped carbon framework, which can

enhance the conductivity and durability of the Fe–Ni active sites. The porous graphitized carbon layer completely encloses the Fe–Ni compound inside, protecting the $FeNi_3$ and $NiFe_2O_4$ active sites without damaging electrical conductivity and mass transfer ability of catalysis. Besides, the graphitic layers are not oriented parallel to the axis direction of NCF and show considerable defects and edges on the surface [154], which can improve the surface affinity for H^+ in the solution.

4. Conclusion

In summary, this mini review briefly introduces the current development status and mainstream obstacles of carbon-based materials used in electrochemical water splitting. For noble metal carbon-based catalysts, confinement pyrolysis and electrochemical modification methods can greatly improve the dispersion of noble metal single atoms or nanoparticles, thus increasing the utilization rate of noble metal atoms and reducing the cost of catalyst without damaging the excellent intrinsic activities and stabilities of noble metals. For non-noble metal catalysts, the coordination environment modification and carbon coating protection strategies can significantly improve the intrinsic activity and endurance of non-noble metal catalysts, respectively. According to the above conclusion, we can combine the two or more strategies mentioned above to create carbon-based catalysts with more comprehensive functions and better performance. For example, we can first create or improve a non-noble metal overall water splitting catalyst that can be stable under acidic by using carbon coating protection strategy. Then we boost its electrocatalytic performance under alkaline conditions by modifying its coordination environment. Finally, an electrocatalyst that can be used in universal pH environment will be obtained. For another example, OER catalyst with excellent performance can be synthesized by using confinement pyrolysis method first, and then Pt can be *in-situ* deposited by electrochemical modification method to enhance its HER performance, so that it can catalyze the overall water splitting reaction. We hope that by combining the above strategies we introduced, we can achieve better performance, better stability, lower cost and more practical carbon-based materials boosting electrochemical water splitting.

Declaration of competing interest

The authors declare that they have no known competing financial interests or personal relationships that could have appeared to influence the work reported in this paper.

Acknowledgments

This work was supported by the Natural Science Foundation of Jilin Province (No. 20200201020JC), Key Research Project of the Education Department of Jilin Province of China (No. JJKH20211046KJ).

References

[1] E. Anagnostou, E.H. John, K.M. Edgar, et al., Nature 533 (2016) 380–384.
[2] B. Obama, Science 355 (2017) 126–129.
[3] H. Schneider Stephen, Science 243 (1989) 771–781.
[4] P. Lu, Y. Yang, J. Yao, et al., Appl. Catal. B: Environ. 241 (2019) 113–119.
[5] D. Larcher, J.M. Tarascon, Nat. Chem. 7 (2015) 19–29.
[6] Y. Mun, K. Kim, S. Kim, et al., Appl. Catal. B: Environ. 236 (2018) 154–161.
[7] K. Kamiya, Chemical Science 11 (2020) 8339–8349.
[8] W. Lubitz, W. Tumas, Chem. Rev. 107 (2007) 3900–3903.
[9] Z. Zhang, L. Cong, Z. Yu, L. Qu, W. Huang, Mater. Today Energy 16 (2020) 100387.
[10] A.Turner John, Science 305 (2004) 972–974.
[11] J. Luo, J.H. Im, T. Mayer Matthew, et al., Science 345 (2014) 1593–1596.
[12] L. Yang, R. Liu, L. Jiao, Adv. Funct. Mater. 30 (2020) 1909618.
[13] J. Wang, W. Cui, Q. Liu, et al., Adv. Mater. 28 (2016) 215–230.
[14] K. Zeng, D. Zhang, Progr. Energy Combust. Sci. 36 (2010) 307–326.
[15] J. Zhang, W. Jia, S. Dang, Y. Cao, J.Colloid Interf. Sci. 560 (2020) 161–168.
[16] Z. Tao, T. Wang, X. Wang, J. Zheng, X. Li, ACS App, Mater. Interfaces 8 (2016) 35390–35397.
[17] J. Huang, C. Du, J. Nie, et al., Electrochim. Acta 326 (2019) 134982.
[18] I.T. McCrum, M.T.M. Koper, Nat. Energy 5 (2020) 891–899.
[19] H.N. Nong, L.J. Falling, A. Bergmann, et al., Nature 587 (2020) 408–413.
[20] X. Liang, L. Shi, Y. Liu, et al., Angew.Chem. Inter. Ed. 58 (2019) 7631–7635.
[21] C. Lei, Q. Zheng, F. Cheng, et al., Adv. Funct. Mater. 30 (2020) 2003000.
[22] C. Lei, S. Lyu, J. Si, et al., ChemCatChem 11 (2019) 5855–5874.
[23] Y. Peng, B. Lu, S. Chen, Adv. Mater. 30 (2018) 1801995.
[24] T.Y. Ma, S. Dai, M. Jaroniec, S.Z. Qiao, J. Am. Chem. Soc. 136 (2014) 13925–13931.
[25] J.Y. Xue, F.L. Li, Z.Y. Zhao, et al., Dalton Transact 48 (2019) 12186–12192.
[26] L. Zhang, I.S. Amiinu, X. Ren, et al., Inorg. Chem. 56 (2017) 13651–13654.
[27] X. Ren, W. Wang, R. Ge, et al., Chem. Commun. 53 (2017) 9000–9003.
[28] D.H. Ha, B. Han, M. Risch, et al., Nano Energy 29 (2016) 37–45.
[29] Y. Zhang, Y. Liu, M. Ma, et al., Chem. Commun. 53 (2017) 11048–11051.
[30] T. Liu, L. Xie, J. Yang, et al., ChemElectroChem 4 (2017) 1840–1845.
[31] X.F. Lu, L. Yu, J. Zhang, X.W. Lou, Adv. Mater. 31 (2019) 1900699.
[32] N. Cheng, L. Ren, G. Casillas, et al., Sustain. Energy Fuels 3 (2019) 1757–1763.
[33] V. Campisciano, M. Gruttadauria, F. Giacalone, ChemCatChem 11 (2019) 90–133.
[34] J. Ke, F. He, H. Wu, et al., Nano-Micro Lett 13 (2020) 24.
[35] G.R. Bolzan, G. Abarca, W.D.G. Gonçalves, et al., Chem. A Eur. J. 24 (2018) 1365–1372.
[36] R.L. Oliveira, C.S. Oliveira, R. Landers, C.R.D. Correia, ChemistrySelect 3 (2018) 535–543.
[37] T. Sun, S. Zhang, L. Xu, D. Wang, Y. Li, Chem. Commun. 54 (2018) 12101–12104.
[38] C. Lei, W. Zhou, Q. Feng, et al., Nano-Micro Lett. 11 (2019) 45.
[39] Z. Zhang, T. Wang, K. Yao, et al., Inorg. Chem. Commun. 116 (2020) 107914.
[40] J. Tian, Q. Liu, A.M. Asiri, X. Sun, J. Am. Chem. Soc. 136 (2014) 7587–7590.
[41] X. Ji, B. Liu, X. Ren, et al., ACS Sustain. Chem. Eng. 6 (2018) 4499–4503.
[42] Z. Zhang, K. Yao, L. Cong, et al., Catal. Sci. Technol. 10 (2020) 1336–1342.
[43] A. Kumar, S. Bhattacharyya, ACS Appl. Mater. Interfaces 9 (2017) 41906–41915.
[44] W. Zhu, R. Zhang, F. Qu, A.M. Asiri, X. Sun, ChemCatChem 9 (2017) 1721–1743.
[45] C.C. Hou, H.F. Wang, C. Li, Q. Xu, Energy Environ. Sci. 13 (2020) 1658–1693.
[46] Y. Liu, Q. Feng, W. Liu, et al., Nano Energy 81 (2021) 105641.
[47] L. Wang, Z. Li, K. Wang, et al., Nano Energy 74 (2020) 104850.
[48] Y. Wang, B. Liu, Y. Liu, et al., Chem. Commun. 56 (2020) 14019–14022.
[49] Z. Zhang, L. Cong, Z. Yu, et al., Mater. Adv. 1 (2020) 54–60.
[50] K.L. Zhou, Z. Wang, C.B. Han, et al., Nat. Commun. 12 (2021) 3783.
[51] K. Jiang, B. Liu, M. Luo, et al., Nat. Commun. 10 (2019) 1743.
[52] J. Zhang, Y. Zhao, X. Guo, et al., Nat. Catal. 1 (2018) 985–992.
[53] Z. Shi, Y. Wang, J. Li, et al., Joule 5 (2021) 2164–2176.
[54] H. Chen, X. Ai, W. Liu, et al., Angew. Chem. Inter. Ed. 58 (2019) 11409–11413.
[55] R.B. Gordon, M. Bertram, T.E. Graedel, Proc. Nat. Acad, Sci 103 (2006) 1209.
[56] L. Cong, K. Yao, S. Zhang, et al., J. Energy Chem. 59 (2021) 715–720.
[57] L. Zhang, Y. Jia, H. Liu, et al., Angew. Chem. Inter. Ed. 58 (2019) 9404–9408.
[58] L. Zhuang, Y. Jia, H. Liu, et al., Angew. Chem. Inter. Ed. 59 (2020) 14664–14670.
[59] Y. Gao, Z. Han, S. Hong, et al., ACS Appl. Energy Mater. 2 (2019) 6071–6077.
[60] R. Kamai, K. Kamiya, K. Hashimoto, S. Nakanishi, Angew. Chem. Inter. Ed. 55 (2016) 13184–13188.
[61] C. Xia, Y. Qiu, Y. Xia, et al., Nat. Chem. (2021) doi.org/, doi:10.1038/s41557-021-00734-x.
[62] G. Dong, M. Fang, H. Wang, et al., J. Mater. Chem. A 3 (2015) 13080–13086.
[63] R. Chen, C. Yang, W. Cai, et al., ACS Energy Lett 2 (2017) 1070–1075.
[64] X. Guo, G. Fang, G. Li, et al., Science 344 (2014) 616–619.
[65] Q. Fu, H. Saltsburg, M. Flytzani-Stephanopoulos, Science 301 (2003) 935–938.
[66] S. Siahrostami, A. Verdaguer-Casadevall, M. Karamad, et al., Nat. Mater. 12 (2013) 1137–1143.
[67] S. Wei, A. Li, J.C. Liu, et al., Nat. Nanotechnol. 13 (2018) 856–861.
[68] X.F. Yang, A. Wang, B. Qiao, et al., Acc. Chem. Res. 46 (2013) 1740–1748.
[69] T. Campbell Charles, C. Parker Stephen, E. Starr David, Science 298 (2002) 811–814.
[70] M.A. Asoro, D. Kovar, Y. Shao-Horn, L.F. Allard, P.J. Ferreira, Nanotechnology 21 (2009) 025701.
[71] S.B. Simonsen, I. Chorkendorff, S. Dahl, et al., J. Am. Chem. Soc. 132 (2010) 7968–7975.
[72] T.W. Hansen, A.T. DeLaRiva, S.R. Challa, A.K. Datye, Acc. Chem. Res. 46 (2013) 1720–1730.
[73] T. Risse, S. Shaikhutdinov, N. Nilius, M. Sterrer, H.J. Freund, Acc. Chem. Res. 41 (2008) 949–956.
[74] A.K. Datye, Q. Xu, K.C. Kharas, J.M. McCarty, Catal. Today 111 (2006) 59–67.
[75] G. Li, R. Jin, Acc.Chem. Res. 46 (2013) 1749–1758.
[76] Y. Nagai, T. Hirabayashi, K. Dohmae, et al., J. Catal. 242 (2006) 103–109.
[77] J. Lu, B. Fu, C. Kung Mayfair, et al., Science 335 (2012) 1205–1208.
[78] Z. Li, R. Yu, J. Huang, et al., Nat. Commun. 6 (2015) 8248.
[79] M. Moliner, J.E. Gabay, C.E. Kliewer, et al., J. Am. Chem. Soc. 138 (2016) 15743–15750.
[80] Y. Chen, S. Ji, Y. Wang, et al., Angew. Chem. Int. Ed. 56 (2017) 6937–6941.
[81] P. Yin, T. Yao, Y. Wu, et al., Angew. Chem. Int. Ed. 55 (2016) 10800–10805.
[82] C. Seitz Linsey, F. Dickens Colin, K. Nishio, et al., Science 353 (2016) 1011–1014.

[83] C. Spöri, J.T.H. Kwan, A. Bonakdarpour, D.P. Wilkinson, P. Strasser, Angew. Chem. Int. Ed. 56 (2017) 5994–6021.
[84] Y. Yao, S. Hu, W. Chen, et al., Nat. Catal. 2 (2019) 304–313.
[85] W. Seh Zhi, J. Kibsgaard, F. Dickens Colin, et al., Science 355 (2017) eaad4998.
[86] T. Reier, M. Oezaslan, P. Strasser, ACS Catal 2 (2012) 1765–1772.
[87] Z. Yu, J. Xu, Y. Li, et al., J. Mater. Chem. 8 (2020) 24743–24751.
[88] J. Xu, Z. Lian, B. Wei, et al., ACS Catal 10 (2020) 3571–3579.
[89] N. Danilovic, R. Subbaraman, K.C. Chang, et al., Angew. Chem. Inter. Ed. 53 (2014) 14016–14021.
[90] G. Li, S. Li, J. Ge, C. Liu, W. Xing, J. Mater. Chem. A 5 (2017) 17221–17229.
[91] S. Siracusano, N. Van Dijk, E. Payne-Johnson, V. Baglio, A.S. Aricò, Appl. Catal. B: Environ. 164 (2015) 488–495.
[92] L. Wang, V.A. Saveleva, S. Zafeiratos, et al., Nano Energy 34 (2017) 385–391.
[93] J. Shan, T. Ling, K. Davey, Y. Zheng, S.Z. Qiao, Adv. Mater. 31 (2019) 1900510.
[94] J. Xu, J. Li, Z. Lian, et al., ACS Catal 11 (2021) 3402–3413.
[95] K.S. Weeraratne, H. El-Kaderi, Y. Lu, Cell Rep. Phys. Sci. 2 (2021) 100495.
[96] S.Y. Ding, J. Gao, Q. Wang, et al., J. Am. Chem. Soc. 133 (2011) 19816–19822.
[97] L. Chen, L. Zhang, Z. Chen, et al., Chem. Sci. 7 (2016) 6015–6020.
[98] K. Kamiya, R. Kamai, K. Hashimoto, S. Nakanishi, Nat. Commun. 5 (2014) 5040.
[99] K. Cui, W. Zhong, L. Li, et al., Small 15 (2019) 1804419.
[100] S. Lu, Y. Hu, S. Wan, et al., J. Am. Chem. Soc. 139 (2017) 17082–17088.
[101] K. Iwase, T. Yoshioka, S. Nakanishi, K. Hashimoto, K. Kamiya, Angew. Chem. Int. Ed. 54 (2015) 11068–11072.
[102] J. Tang, J. Liu, C. Li, et al., Angew. Chem. Int. Ed. 54 (2015) 588–593.
[103] H. Zhang, P. An, W. Zhou, et al., Sci. Adv. 4 (2021) eaao6657.
[104] S. Cherevko, A.R. Zeradjanin, G.P. Keeley, K.J.J. Mayrhofer, J. Electrochem. Soc. 161 (2014) H822–H830.
[105] S. Cherevko, A.R. Zeradjanin, A.A. Topalov, et al., ChemCatChem 6 (2014) 2219–2223.
[106] D.C. Johnson, D.T. Napp, S. Bruckenstein, Electrochim. Acta 15 (1970) 1493–1509.
[107] P.J. Kulesza, W. Lu, L.R. Faulkner, J. Electroanal. Chem. 336 (1992) 35–44.
[108] A.A. Topalov, S. Cherevko, A.R. Zeradjanin, et al., Chem. Sci. 5 (2014) 631–638.
[109] L. Xing, M.A. Hossain, M. Tian, et al., Electrocatalysis 5 (2014) 96–112.
[110] M. Tavakkoli, N. Holmberg, R. Kronberg, et al., ACS Catal 7 (2017) 3121–3130.
[111] K.L. Zhou, C. Wang, Z. Wang, et al., Energy Environm. Sci. 13 (2020) 3082–3092.
[112] L. Zhang, J.M.T.A. Fischer, Y. Jia, et al., J. Am. Chem. Soc. 140 (2018) 10757–10763.
[113] R.K. Das, Y. Wang, S.V. Vasilyeva, et al., ACS Nano 8 (2014) 8447–8456.
[114] L. Zhang, L. Han, H. Liu, X. Liu, J. Luo, Angew. Chem. Int. Ed. 56 (2017) 13694–13698.
[115] Y. Tan, H. Wang, P. Liu, et al., Adv. Mater. 28 (2016) 2951–2955.
[116] D.A.J. Rand, R. Woods, J. Electroanal. Chem. Interfac. Electrochem. 35 (1972) 209–218.
[117] D. Kong, J.J. Cha, H. Wang, H.R. Lee, Y. Cui, Energy Environ. Sci. 6 (2013) 3553–3558.
[118] J.O.M. Bockris, Inter. J. Hydrogen Energy 27 (2002) 731–740.
[119] A. Mendoza-Garcia, H. Zhu, Y. Yu, et al., Angew. Chem. Int. Ed. 54 (2015) 9642–9645.
[120] Y. Yuan, Y. Lu, B.-E. Jia, et al., Nano-Micro Lett. 11 (2019) 42.
[121] L. Xie, F. Qu, Z. Liu, et al., J. Mater. Chem. A 5 (2017) 7806–7810.
[122] W.-F. Chen, K. Sasaki, C. Ma, et al., Angew. Chem. Int. Ed. 51 (2012) 6131–6135.
[123] S. Li, J. Sun, J. Guan, Chin. J. Catal. 42 (2021) 511–556.
[124] J. Xie, J. Zhang, S. Li, et al., J. Am. Chem. Soc. 135 (2013) 17881–17888.
[125] Z.W. Seh, K.D. Fredrickson, B. Anasori, et al., ACS Energy Lett. 1 (2016) 589–594.
[126] A. Kumar, V.K. Vashistha, D.K. Das, et al., Fuel 304 (2021) 121420.
[127] H. Wu, H. Li, X. Zhao, et al., Energy Environ. Sci. 9 (2016) 3736–3745.
[128] P. Chen, T. Zhou, L. Xing, et al., Angew. Chem. Int. Ed. 56 (2017) 610–614.
[129] Y. Liu, H. Jiang, Y. Zhu, X. Yang, C. Li, J. Mater. Chem. A 4 (2016) 1694-1701.
[130] H.-W. Liang, S. Brüller, R. Dong, et al., Nat. Commun. 6 (2015) 7992.
[131] P. Munnik, P.E. de Jongh, K.P. de Jong, Chem. Rev. 115 (2015) 6687–6718.
[132] H. Fei, J. Dong, Y. Feng, et al., Nat. Catal. 1 (2018) 63–72.
[133] L. Chai, Z. Hu, X. Wang, et al., Adv. Sci. 7 (2020) 1903195.
[134] L. Yan, H. Wang, J. Shen, et al., Chem. Eng. J. 403 (2021) 126385.
[135] X. Feng, X. Bo, L. Guo, J. Power Sources 389 (2018) 249–259.
[136] J. Yang, X. Wang, B. Li, et al., Adv. Funct. Mater. 27 (2017) 1606497.
[137] J. Jin, J. Yin, H. Liu, et al., ChemCatChem 11 (2019) 2780–2792.
[138] D. Banham, S. Ye, K. Pei, et al., J. Power Sources 285 (2015) 334–348.
[139] J.A. Varnell, E.C.M. Tse, C.E. Schulz, et al., Nat. Commun. 7 (2016) 12582.
[140] C.H. Choi, C. Baldizzone, J.-P. Grote, et al., Angew. Chem. Int. Ed. 54 (2015) 12753–12757.
[141] C.H. Choi, C. Baldizzone, G. Polymeros, et al., ACS Catal 6 (2016) 3136–3146.
[142] V. Goellner, V. Armel, A. Zitolo, E. Fonda, F. Jaouen, J. Electrochem. Soc. 162 (2015) H403–H414.
[143] J. Herranz, F. Jaouen, M. Lefèvre, et al., J. Phys. Chem. C 115 (2011) 16087–16097.
[144] B.Y. Xia, Y. Yan, N. Li, et al., Nat. Energy 1 (2016) 15006.
[145] Y. He, S. Hwang, D.A. Cullen, et al., Energy Environ. Sci. 12 (2019) 250–260.
[146] J. Gao, K. Ye, L. Yang, et al., Inorganic Chem 53 (2014) 691–693.
[147] I.S. Amiinu, X. Liu, Z. Pu, et al., Adv. Funct. Mater. 28 (2018) 1704638.
[148] T. Xing, Y. Lou, Q. Bao, J. Chen, CrystEngComm 16 (2014) 8994–9000.
[149] Y. Chang, F. Hong, C. He, Q. Zhang, J. Liu, Adv. Mater. 25 (2013) 4794–4799.
[150] M. Jiang, X. Cao, D. Zhu, Y. Duan, J. Zhang, Electrochim. Acta 196 (2016) 699–707.
[151] L. Zhang, C. Lu, F. Ye, et al., Adv. Mater. 33 (2021) 2007523.
[152] Y. Liu, H. Cheng, M. Lyu, et al., J. Am. Chem. Soc. 136 (2014) 15670–15675.
[153] D. Kong, H. Wang, Z. Lu, Y. Cui, J. Am. Chem. Soc. 136 (2014) 4897–4900.
[154] X. Zhao, P. Pachfule, S. Li, et al., Angew. Chem. Int. Ed. 57 (2018) 8921–8926.